MET O 11 TECHNICAL NOTE NO. 109

A versatile limited area sigma coordinate model - preliminary results showing the affect on forecast rainfall of changing the resolution.

by

R S BELL

Meteorological Office (Met O 11)
London Road
Bracknell, Berkshire
United Kingdom

JULY 1978

1. Introduction

This model has been developed as a flexible aid to further research into short range forecasting of dynamical systems affecting the detailed weather over the UK. The model is based on the fine mesh version of the Meteorological Office 10-level numerical weather prediction model (Burridge and Gadd 1977). It differs from the model described by Burridge and Gadd in several aspects. Firstly sigma coordinates have been used instead of pressure coordinates. This provides for a more realistic treatment of topography and the lower boundary condition. Comparisons of the two coordinate systems (Temperton 1976) indicate that the use of sigma coordinates improves the forecast in terms of r.m.s. errors. The formulation of the dynamical equations in terms of sigma coordinates is identical to that used by Temperton. Secondly the split explicit finite difference scheme (Gadd 1976) has been used. Browne (1978) has recently incorporated this scheme into the fine-mesh version of the 10-level model.

The model has been programmed so that the number and spacing of the grid points in both the horizontal and the vertical may be easily changed. Thus as well as allowing for changes in horizontal and vertical resolution, the area covered by the model can also be changed and the vertical levels may be unequally spaced.

Further work needs to be done before any definite conclusions can be drawn as to the improvement in the PMSL forecast.

However several interesting results have been obtained with regard to rainfall forecasts and these will be presented here.

2. Equations

a. The basic equations

Notation -

Coordinate system, (x, y, σ)

wind components, $= (u, V)$

potential temperature, θ

humidity mixing ratio, r

surface pressure p_*

$$\dot{\sigma} = \frac{d\sigma}{dt} \; ; \quad \sigma = \frac{p}{p_*} \; ; \quad \phi = gz \; ; \quad \Pi = \left(\frac{p}{p_{1000}}\right)^{\kappa} ;$$

$$\hat{\underline{V}} = \int_0^1 \underline{V}\, d\sigma \; ; \quad \underline{V}' = \underline{V} - \hat{\underline{V}} \; ; \quad \xi = \mathrm{curl}\, \underline{V} \; ; \quad E = \tfrac{1}{2}|\underline{V}|^2 .$$

The basic adiabatic inviscid equations are divided into an adjustment stage and an advection stage as follows.

i. Adjustment

$$\frac{\partial \underline{V}}{\partial t} + \dot{\sigma}\frac{\partial \underline{V}}{\partial \sigma} + f\underline{k}\times\underline{V} + \nabla\phi + c_p\theta\nabla\Pi = 0 \qquad (1)$$

$$\frac{\partial \theta}{\partial t} + \dot{\sigma}\frac{\partial \theta}{\partial \sigma} = 0 \qquad (2)$$

$$\frac{\partial r}{\partial t} + \dot{\sigma}\frac{\partial r}{\partial \sigma} = 0 \qquad (3)$$

$$\frac{\partial p_*}{\partial t} + \mathrm{div}(\hat{\underline{V}}\, p_*) = 0 \qquad (4)$$

The diagnostic hydrostatic and continuity equations are also used in the adjustment stage

$$\frac{\partial \phi}{\partial \sigma} + c_p\theta\frac{\partial \Pi}{\partial \sigma} = 0 \qquad (5)$$

$$p_*\frac{\partial \dot{\sigma}}{\partial \sigma} + \mathrm{div}(\underline{V}' p_*) = 0 \qquad (6)$$

ii. Advection

$$\frac{\partial \underline{V}}{\partial t} + \xi\underline{k}\times\underline{V} + \nabla E = 0 \qquad (7)$$

$$\frac{\partial \theta}{\partial t} + \underline{V}\cdot\nabla\theta = 0 \qquad (8)$$

$$\frac{\partial r}{\partial t} + \underline{V}\cdot\nabla r = 0 \qquad (9)$$

The variables are staggered in the horizontal as follows:-

```
o       o       o

    x       x

o       o       o

    x       x

o       o       o
```

$p_*, \theta, r, \dot{\sigma}, \phi, m_1$ are calculated at points marked o

and $\underline{V} = (u, v)$, m_2 are calculated at points marked X

where m is the map factor.

In the vertical

u, v, θ, ϕ, r are calculated at the main sigma levels

$\dot{\sigma}$ is calculated at levels midway between the main levels.

b. Finite Difference Equations

The equations in finite difference form are given in terms of the following notation

(i) the velocity is carried as $\underline{V}^* = \underline{V}/m$

(ii) $(\delta_x A)_i = (A_{i+\frac{1}{2}} - A_{i-\frac{1}{2}})/\Delta i$

(iii) $\overline{A_i}^x = (A_{i+\frac{1}{2}} + A_{i-\frac{1}{2}})/2$

where for horizontal derivatives $\Delta i = a$, the gridlength at the North pole and for vertical derivatives $\Delta_i = \Delta\sigma_i$ (which may be different for each level).

i. Adjustment

$$\frac{\partial u^*}{\partial t} = f v^* - \overline{\delta_x \phi}^y - c_p \overline{\overline{\theta}^x \delta_x \Pi}^y - \overline{\overline{\dot{\sigma}}^{xy} \delta_\sigma u^*}^\sigma \quad (10)$$

$$\frac{\partial v^*}{\partial t} = -f u^* - \overline{\delta_y \phi}^x - c_p \overline{\overline{\theta}^y \delta_y \Pi}^x - \overline{\overline{\dot{\sigma}}^{xy} \delta_\sigma v^*}^\sigma \quad (11)$$

$$\frac{\partial \theta}{\partial t} = - \overline{\dot{\sigma} \delta_\sigma \theta}^\sigma \quad (12)$$

$$\frac{\partial r}{\partial t} = - \overline{\dot{\sigma} \delta_\sigma r}^\sigma \quad (13)$$

$$\frac{\partial p_*}{\partial t} = - m_1^2 [\overline{\delta_x (p_*^{xy} \hat{u}^*)}^y + \overline{\delta_y (p_*^{xy} \hat{v}^*)}^x] \quad (14)$$

hydrostatic equation $\delta_\sigma \phi = -c_p \Pi_* \overline{\theta}^\sigma \delta_\sigma (\sigma^\kappa)$ (15)

continuity equation $p_* \delta_\sigma \dot{\sigma} = -m_1^2 [\overline{\delta_x (\overline{p}_*^{xy} u^*)}^y + \overline{\delta_y (\overline{p}_*^{xy} v^*)}^x]$ (16)

ii. Advection

$$\frac{\partial u^*}{\partial t} = m_1^2 (\overline{\delta_x v^*}^y - \overline{\delta_y u^*}^x) \overline{v^*}^{xy} - \delta_x [\overline{\tfrac{1}{2} m_2^2 (u^{*2} + v^{*2})}^y] \quad (17)$$

$$\frac{\partial v^*}{\partial t} = -m_1^2 (\overline{\delta_x v^*}^y - \overline{\delta_y u^*}^x) \overline{u^*}^{xy} - \delta_y [\overline{\tfrac{1}{2} m_2^2 (u^{*2} + v^{*2})}^x] \quad (18)$$

$$\frac{\partial \theta}{\partial t} = -m_2^2 (u^* \overline{\delta_x \theta}^y + v^* \overline{\delta_y \theta}^x) \quad (19)$$

$$\frac{\partial r}{\partial t} = -m_2^2 (u^* \overline{\delta_x r}^y + v^* \overline{\delta_y r}^x) \quad (20)$$

More complicated differences are used for improved phase speeds in the second step of the two-step advection integration scheme (fourth-order differencing). In the second step equations 17-20 differ due to the staggering in time (m_1 and m_2 are interchanged).

c. Integration scheme

i. Adjustment

$$\theta_{n+1} = \theta_n + \left(\frac{\partial\theta}{\partial t}\right)_n \delta t \tag{21}$$

$$r_{n+1} = r_n + \left(\frac{\partial r}{\partial t}\right)_n \delta t \tag{22}$$

$$p_{*n+1} = p_{*n} + \left(\frac{\partial p_*}{\partial t}\right)_n \delta t \tag{23}$$

$$\underline{V}^*_{n+1} = \underline{V}^*_n + \left(\frac{\partial \underline{V}^*}{\partial t}\right)_{n,n+1} \delta t \tag{24}$$

The tendency $\left(\frac{\partial V}{\partial t}\right)_{n,n+1}$ is calculated using V_n, $\dot{\sigma}_n$, ϕ_{n+1}, θ_{n+1}, Π_{n+1}

ii. Advection

A two-step Lax Wendroff integration scheme is used.

$$\theta_{n+\frac{1}{2}} = \overline{\theta}_n^{xy} + \tfrac{1}{2}\Delta t\left(\frac{\partial\theta}{\partial t}\right)_n \tag{25}$$

$$\theta_{n+1} = \theta_n + \Delta t\left(\frac{\partial\theta}{\partial t}\right)_{n+\frac{1}{2}} \tag{26}$$

and similarly for the other variables.

The adjustment stage is integrated three times using a time step δt; the advection stage is integrated once with a time step $\Delta t = 3\delta t$.

The charge in $\underline{V}$ due to friction and the change in due to physical processes are added on after the advection step. The change in r due to physical processes is calculated once per advection step and a third of the change is added on after every adjustment step.

3. General Results

One case was chosen for study, data time 12Z 4 January 1978. An active baroclinic zone existed in Mid-Atlantic and depressions were evolving in the Iceland region. A deep low off Cape Farewell and an anticyclone near Biscay were progressing slowly eastward. Figure 1 shows the initial PMSL field.

Three different configurations were tested, these were

a. 9 levels (σ = .15 to .95 step .1), 100 km spacing

b. 18 levels (σ = .15 to .95 step .05), 100 km spacing

c. 9 levels (σ = .15 to .95 step .1), 50 km spacing

Forecasts a. and b. were run to 24 hours.

Forecast c. was run to 12 hours.

The initial fields are derived by interpolation from the initialised data used for the pressure model forecasts. No initialisation is carried out on the sigma surfaces. This has caused a few minor problems. Instabilities which developed when a level was introduced above .1σ are probably due to incorrect extrapolation from 100 mb data. Also throughout the forecast there appears to be a loss of mass and the reasons for this are still being investigated.

Several other points are worth noting. A timestep of 10 minutes was used for the 100 km forecasts. A 5 minute timestep was too large however for the 50 km forecast and a 4 minute timestep was used instead. (A trial with a 5 minute timestep but 4 adjustments per advection stage also gave satisfactory results). The boundary scheme currently being used is a simple imposition of the values of P_*, u, v, θ, r on the boundary. It appears some improvement is required here.

Comparison of PMSL charts (see Figures 2a, 2b, 3a, 4a, 5a, 5b, 6) show no major differences in the forecasts.

A greater improvement might be expected had the initial data for the two improved resolution versions contained more information. In this study the data was obtained by interpolation from 100 km, 10 level data.

4. Rainfall comparisons

There is as yet no deep convection scheme; the convective processes are handled by convective adjustment. The rainfall resulting from the forecast is nearly all dynamic in origin.

The comparison will be considered in three sections

a. (9 level, 100 km) - (18 level, 100 km)

b. (9 level, 100 km) - (9 level, 50 km)

c. (9 level, 100 km) - (Operational fine mesh model 10 level, 100 km)

a. There is little significant difference between these two forecasts. Figures 2b and 3a show 24 hour PMSL forecasts and Figures 2d and 3b show 24 hour rainfall accumulations. The distribution of accumulated rainfall is very similar in both forecasts although amounts are marginally less from the 18 level forecast. We must not conclude from this first experiment that improving the vertical resolution is not beneficial; the use of actual instead of interpolated data and also improved physical parameterisation might effect the results.

b. Comparing Figures 2a and 4a which show 12 hour PMSL, and Figures 2c and 4b which show 12 hour rainfall accumulations, we see that although there is hardly any difference in the pressure fields, the rainfall accumulations are considerably different. The three main areas of precipitation are forecast to be 32.6 mm, 18.4 mm and 19.6 mm by the 50 km forecast compared with 23.6 mm, 12.2mm and 14.3 mm by the 100 km forecast.
This is an increase in precipitation of over 40%. Recent results from researchers in the United States have shown similar improvements in precipitation amount by reducing the grid length. See, for example, (Miyakoda and Rosati, 1977) and (Shuman, 1978). It is also interesting to note that the 50 km forecast is significantly more detailed.

c. Comparisons with the current operational model (see Figures 2 and 5) are complicated because the latter includes a deep convection scheme which had the effect of reducing dynamic rainfall. Several differences do stand out however, notably the absence of a precipitation area in the S.W. corner of the chart of the sigma forecast at 24 hours. This is not a bad thing as the rain area in that position from the p-model does not appear to be related to any feature on the chart and may be a spurious boundary affect. Also the rain area off Scandanavia is more intense on the sigma forecast charts, otherwise the main features are similar.

5. Conclusions

Further work is obviously required before the model is satisfactory. Also testing of the model on other case studies and comparison with actual data is necessary.

However the initial results are encouraging especially the rainfall results from the 50 km resolution forecast.

Figures

References

Browne N R	1978	Report on the split explicit rectangle Met O 2b Tech Note No.55.
Burridge D M and Gadd A J	1977	Meteorological Office operational 10 level numerical weather prediction model (Dec 1975). Met Office Sci.Pap.34.
Gadd A J	1976	Progress Report on the split explicit integration scheme. Met O 2b Tech Note No.22
Miyakoda and Rosati	1977	One way nested grid models, the interface conditions and numerical accuracy. MWR 105 p.1092.
Shuman	1978	Numerical Weather Prediction. Bull A.M.S. 59 No.1.
Temperton C	1976	Comparison between pressure and sigma coordinate versions of the 10 level model. Met O 2b Tech Note 29

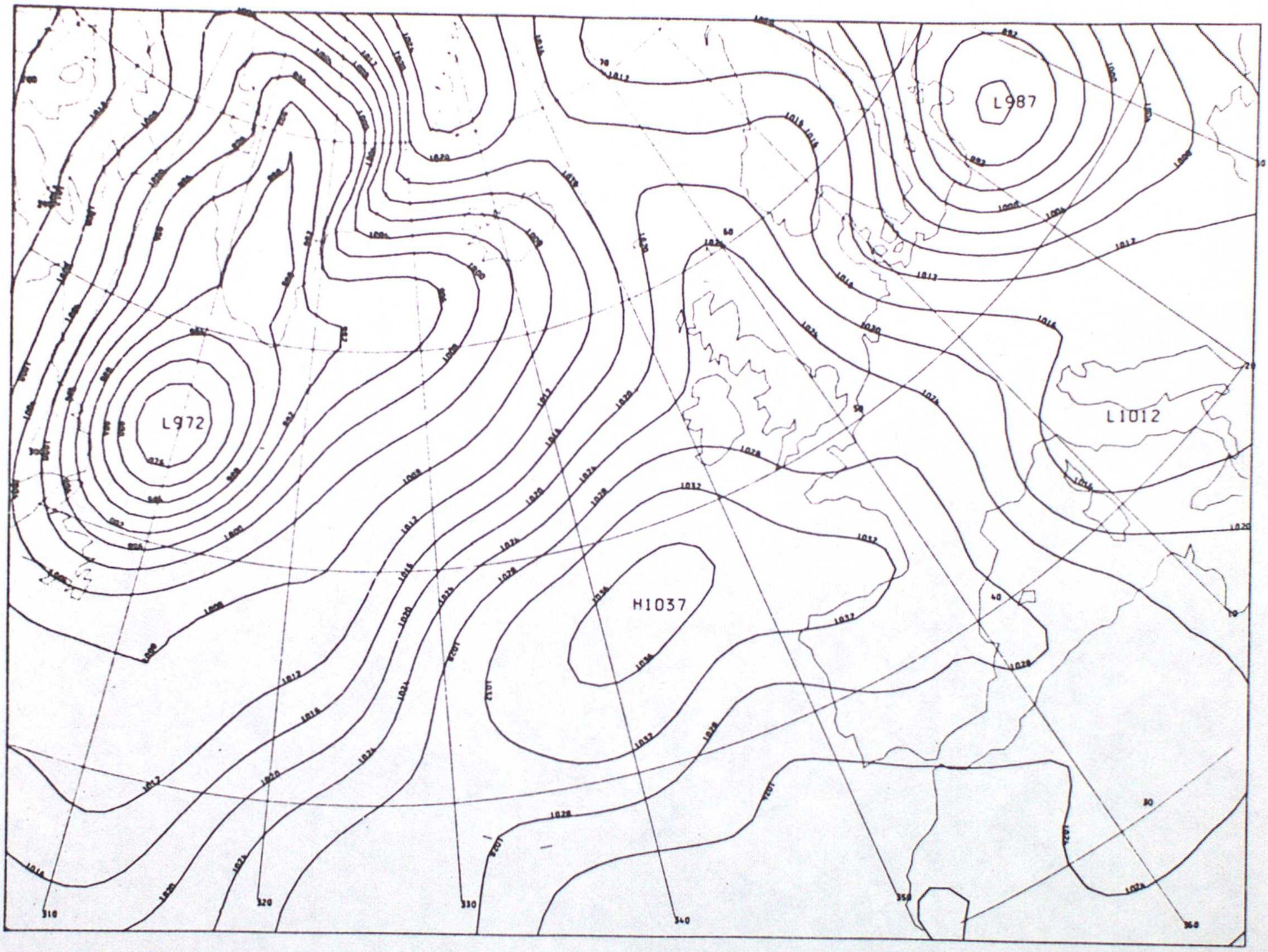

SIGMA SPLIT EXPLICIT
MEAN SEA LEVEL PRESSURE
O HR F/C DATA TIME 12Z 4/1/78

(INITIALISATION)

FIGURE 1

SIGMA SPLIT EXPLICIT
MEAN SEA LEVEL PRESSURE
12 HR F/C DATA TIME 12Z 4/1/78
9 LEVELS 100 KMS

FIGURE 2a

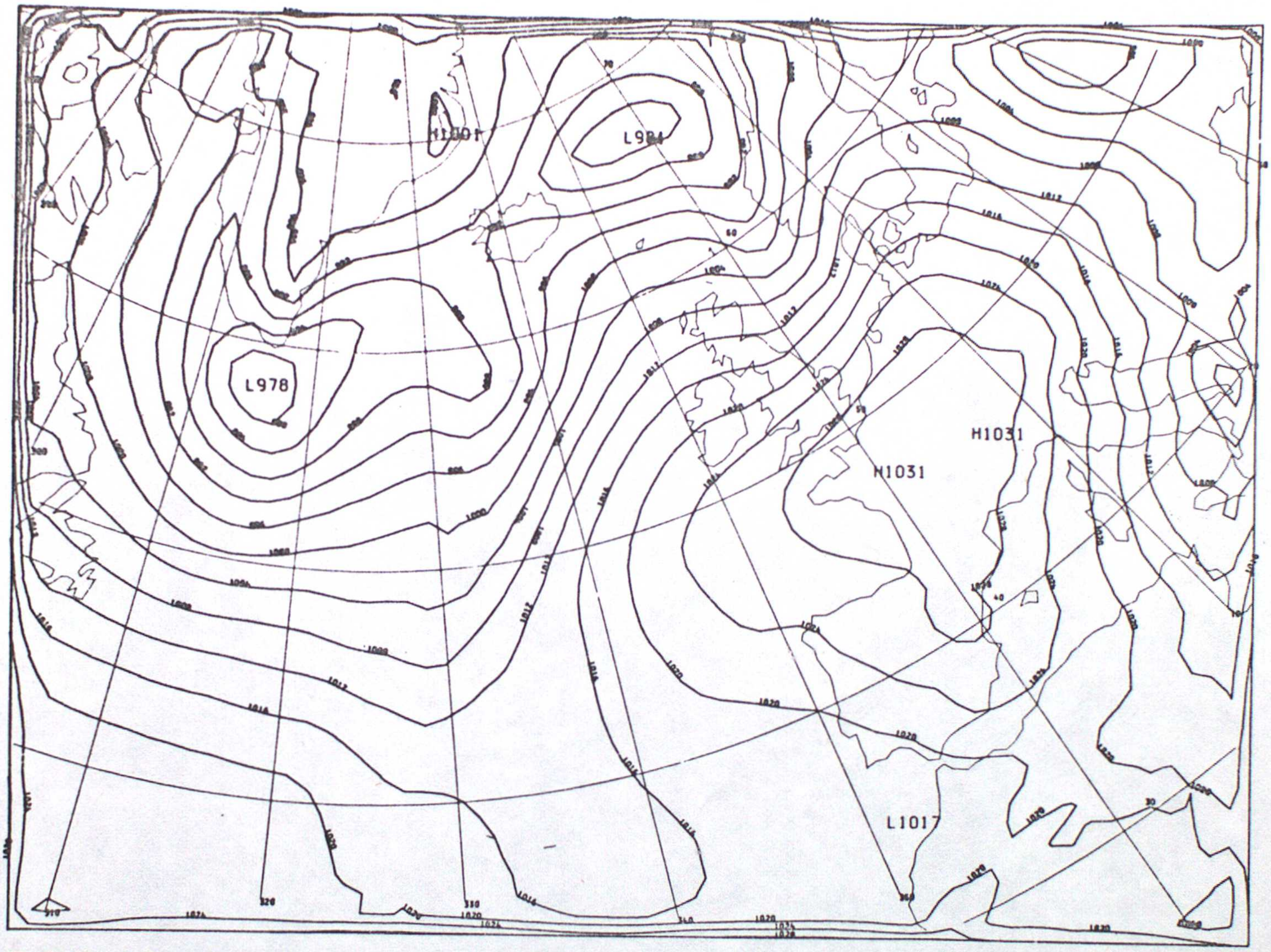

SIGMA SPLIT EXPLICIT
MEAN SEA LEVEL PRESSURE
24 HR F/C DATA TIME 12Z 4/1/78
9 LEVELS 100 KMS

FIGURE 2b

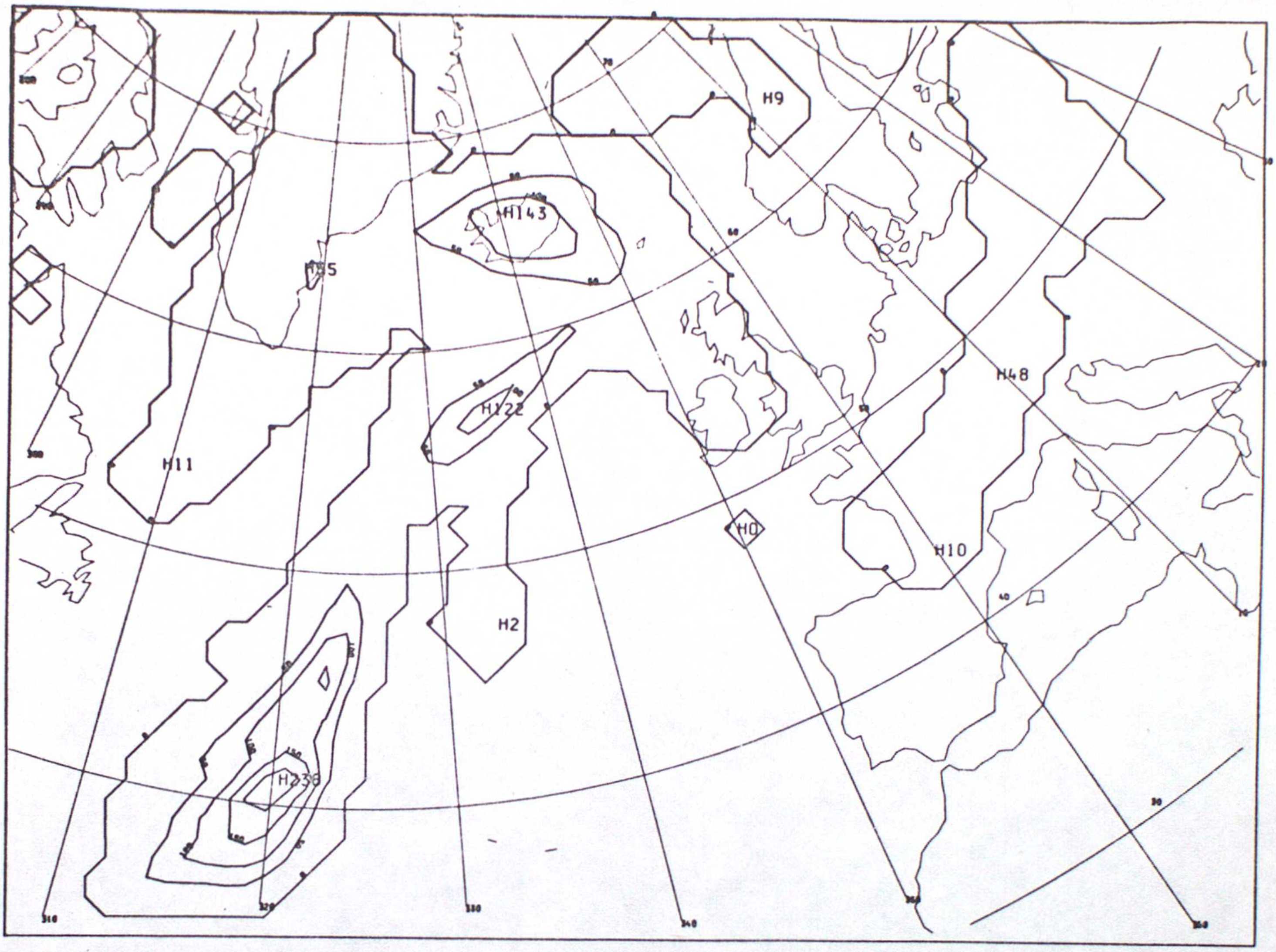

SIGMA SPLIT EXPLICIT
ACC DYN PPN 1/10MM
12 HR F/C DATA TIME 12Z 4/1/78
9 LEVELS 100 KMS

FIGURE 2c

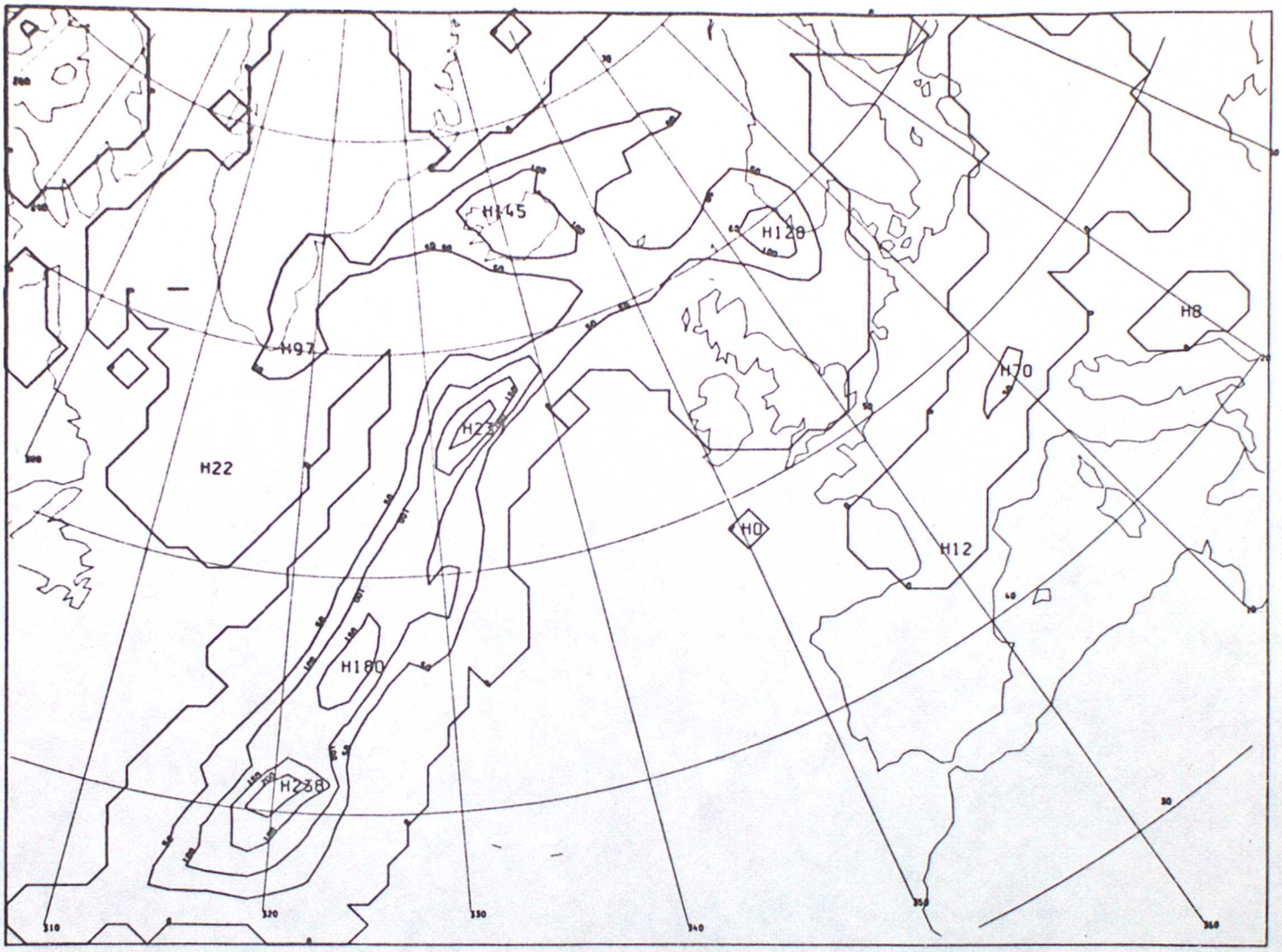

SIGMA SPLIT EXPLICIT
ACC DYN PPN 1/10MM
24 HR F/C DATA TIME 12Z 4/1/78
9 LEVELS 100 KMS

FIGURE 2d

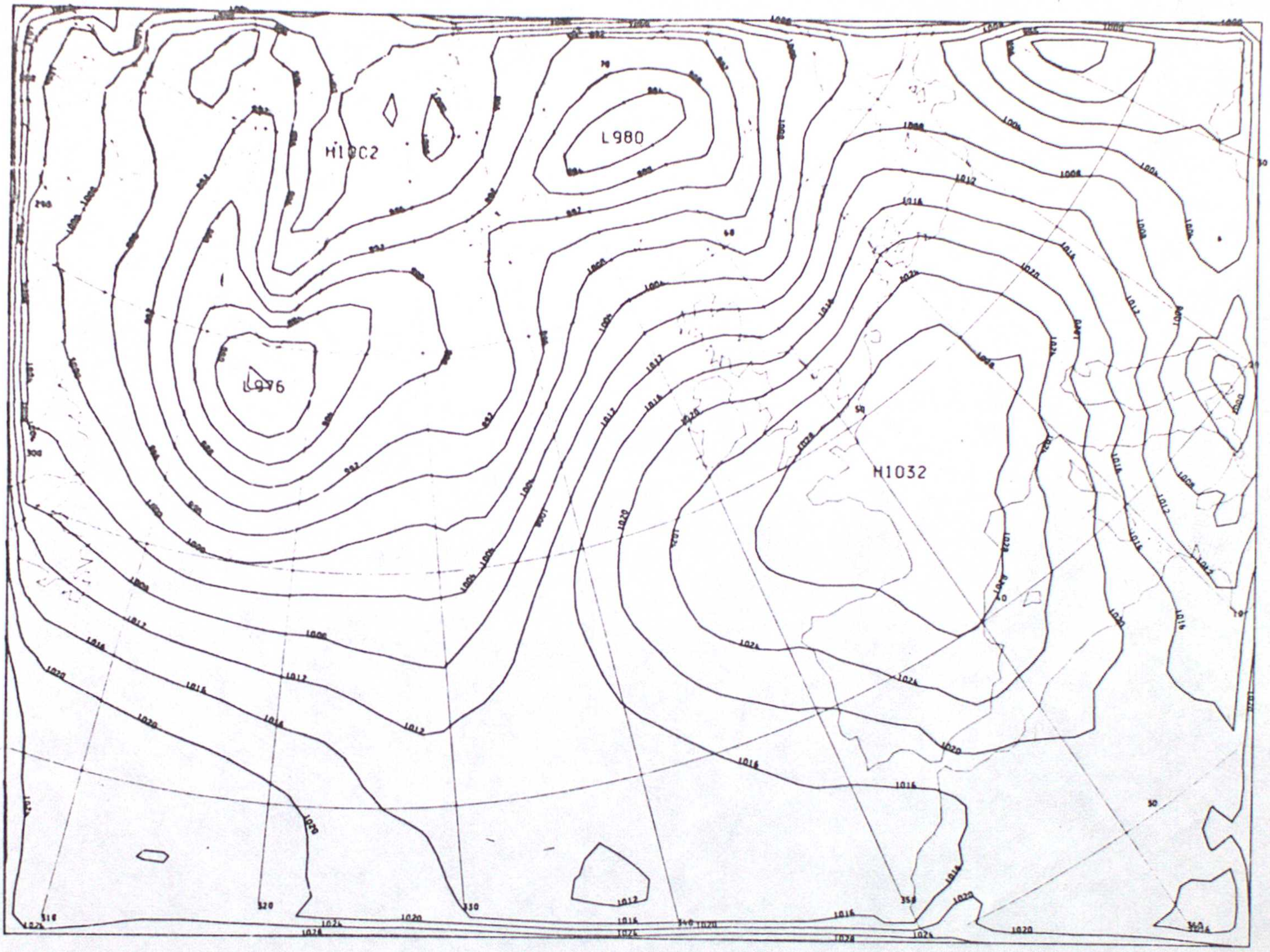

SIGMA SPLIT EXPLICIT
MEAN SEA LEVEL PRESSURE
24 HR F/C DATA TIME 12Z 4/1/78
18 LEVELS 100 KMS

FIGURE 3a

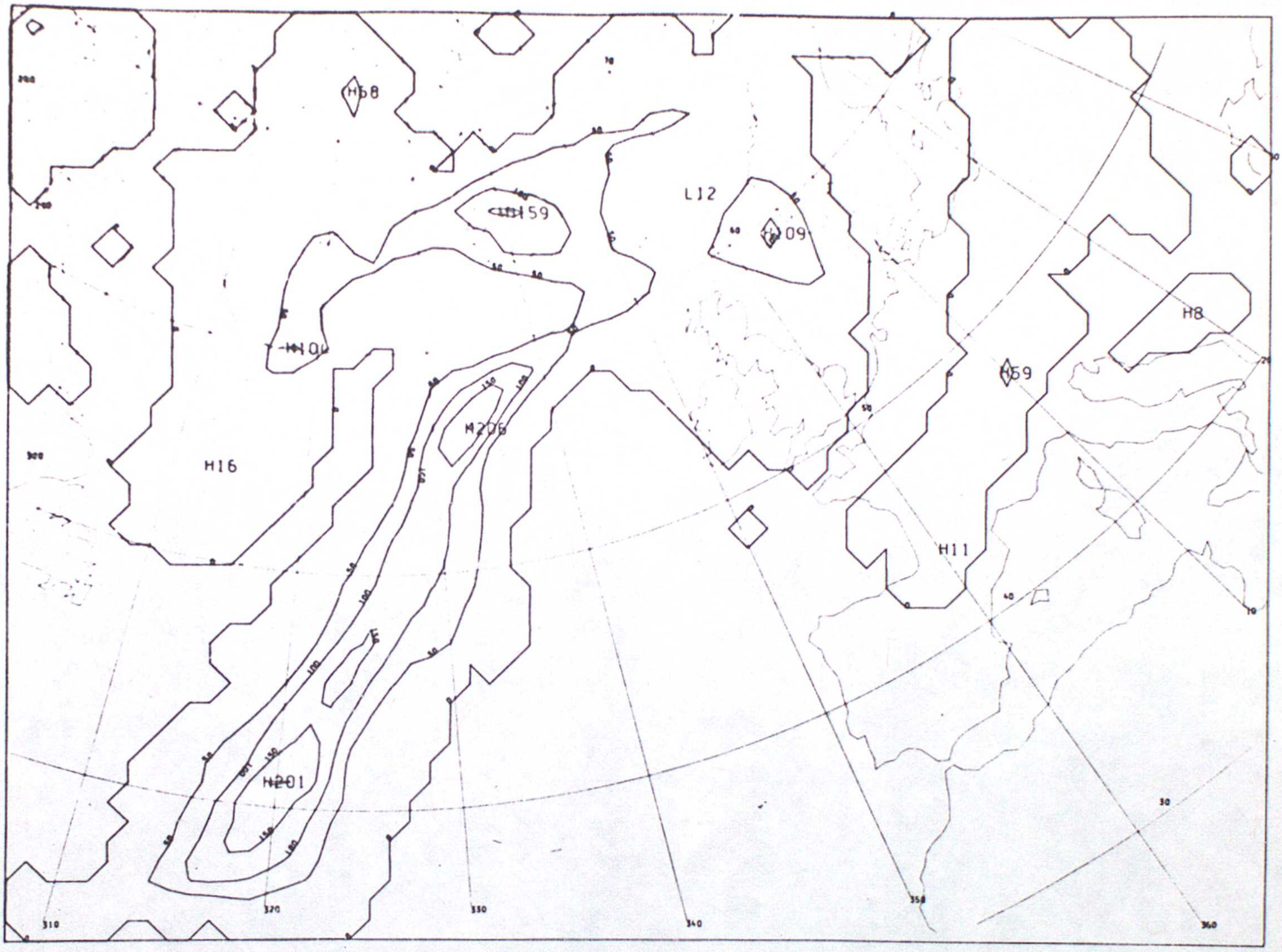

SIGMA SPLIT EXPLICIT
ACC DYN PPN 1/10MM
24 HR F/C DATA TIME 12Z 4/1/78
18 LEVELS 100 KMS

FIGURE 3b

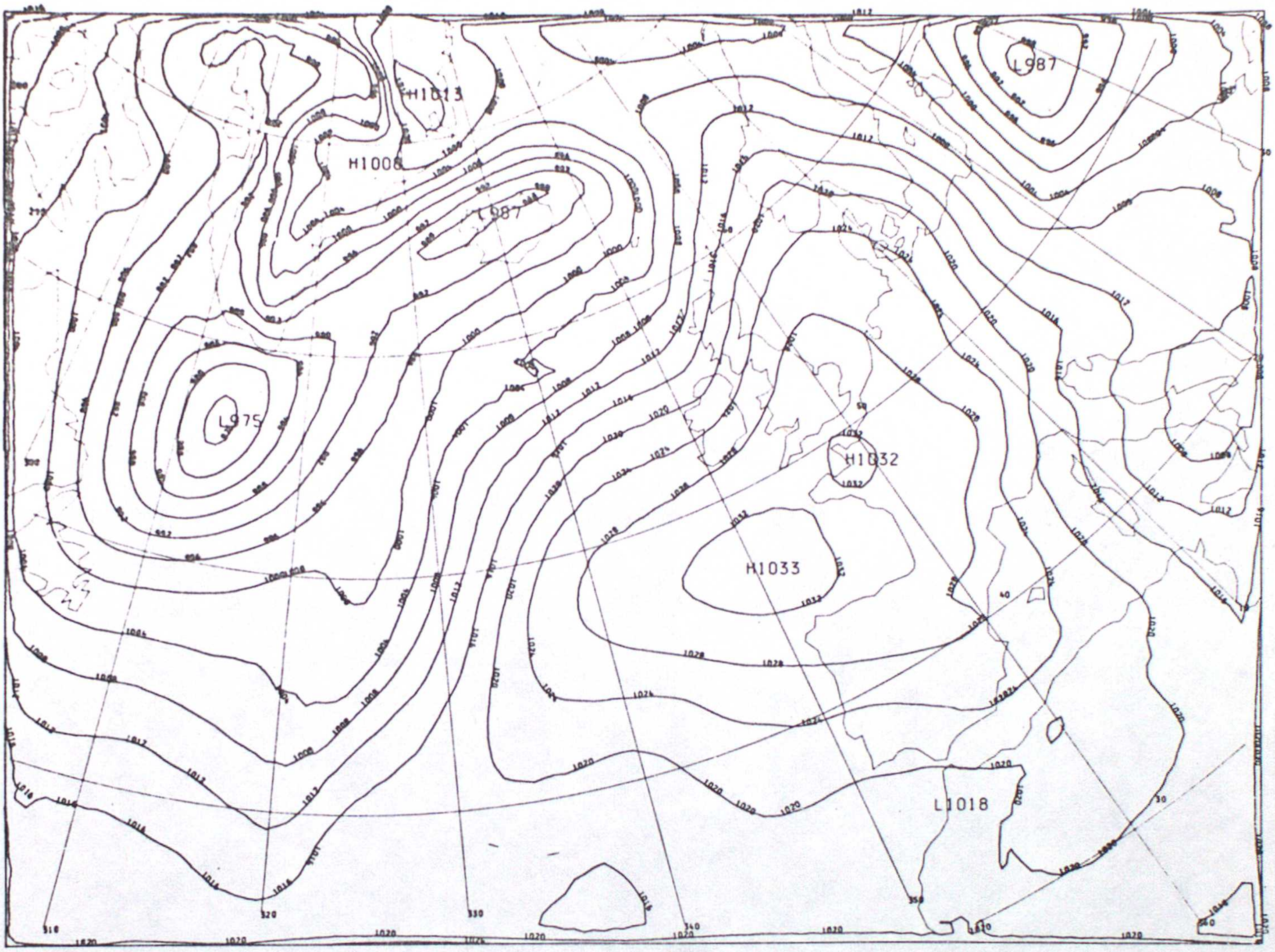

SIGMA SPLIT EXPLICIT
MEAN SEA LEVEL PRESSURE
12 HR F/C DATA TIME 12Z 4/1/78
9LVL,50KM

FIGURE 4a

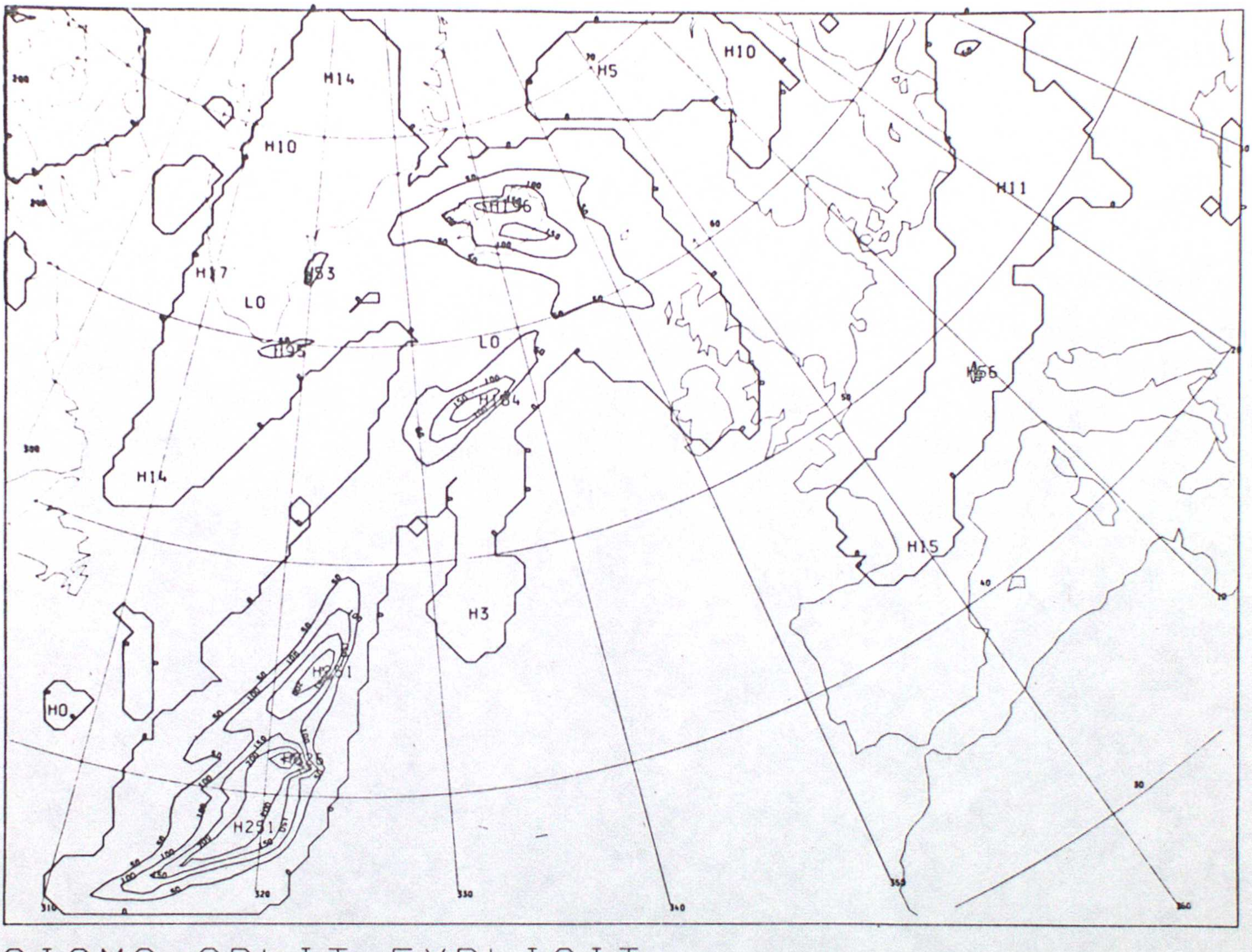

SIGMA SPLIT EXPLICIT
ACC DYN PPN 1/10MM
12 HR F/C DATA TIME 12Z 4/1/78
9LVL,50KM

FIGURE 4b

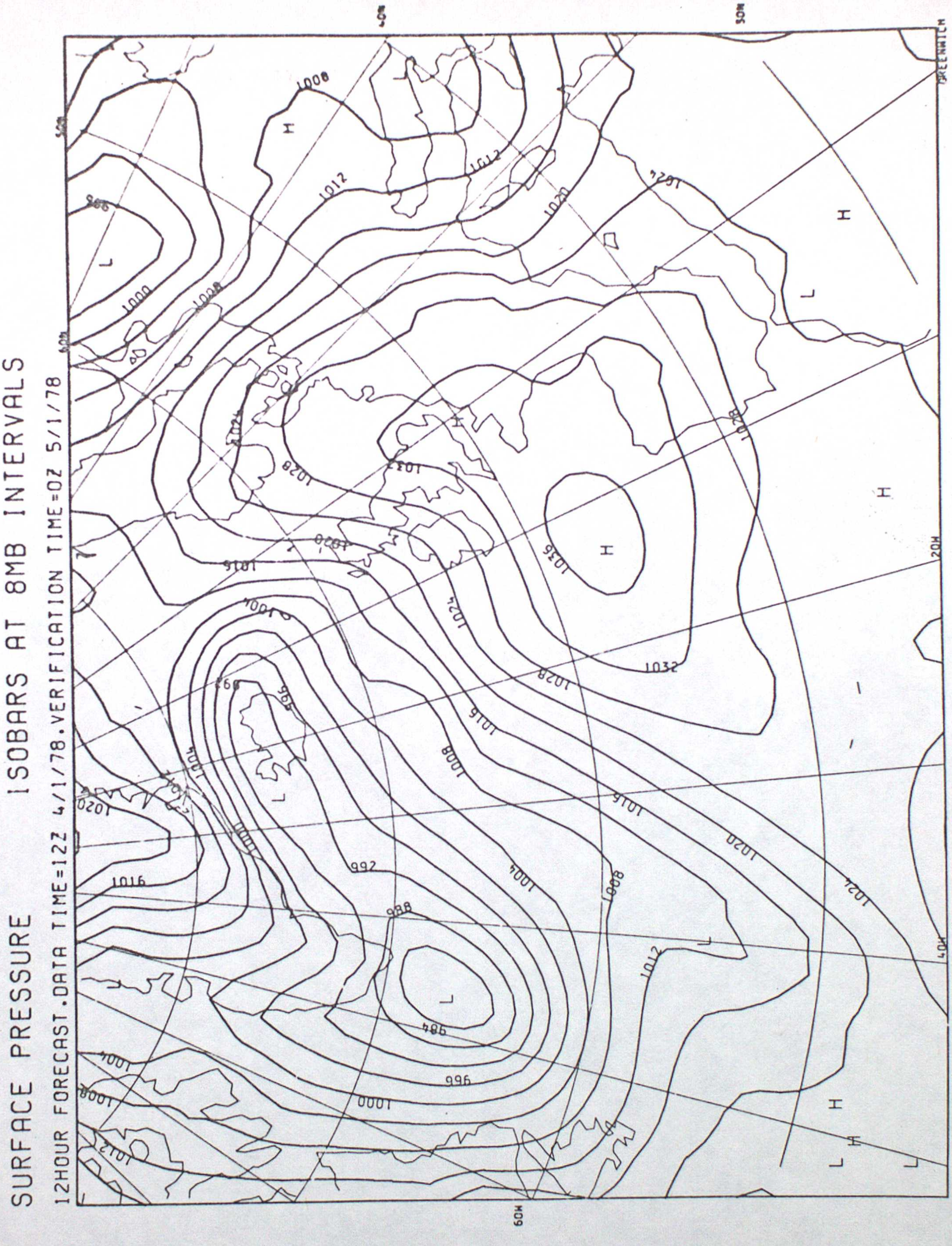
SURFACE PRESSURE ISOBARS AT 8MB INTERVALS
12HOUR FORECAST.DATA TIME=12Z 4/1/78.VERIFICATION TIME=0Z 5/1/78
GREENWICH

FIGURE 5a

SURFACE PRESSURE   ISOBARS AT 8MB INTERVALS

24HOUR FORECAST.DATA TIME=12Z 4/1/78.VERIFICATION TIME=12Z 5/1/78

FIGURE 5b

ACCUMULATED RAIN   ISOHYETS AT 2 MM INTERVALS

12HOUR FORECAST.DATA TIME=12Z 4/1/78.VERIFICATION TIME=0Z 5/1/78

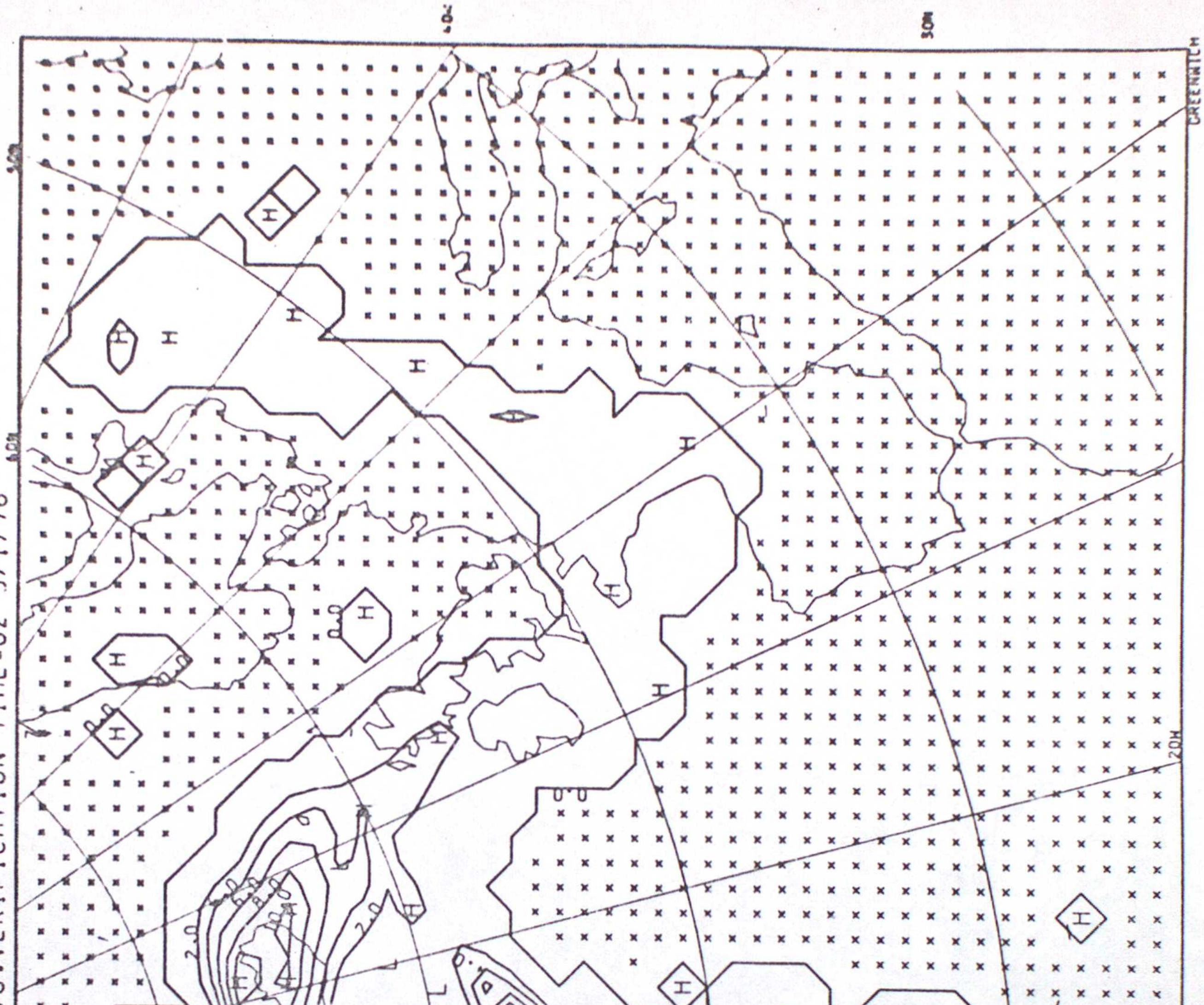

FIGURE 5c

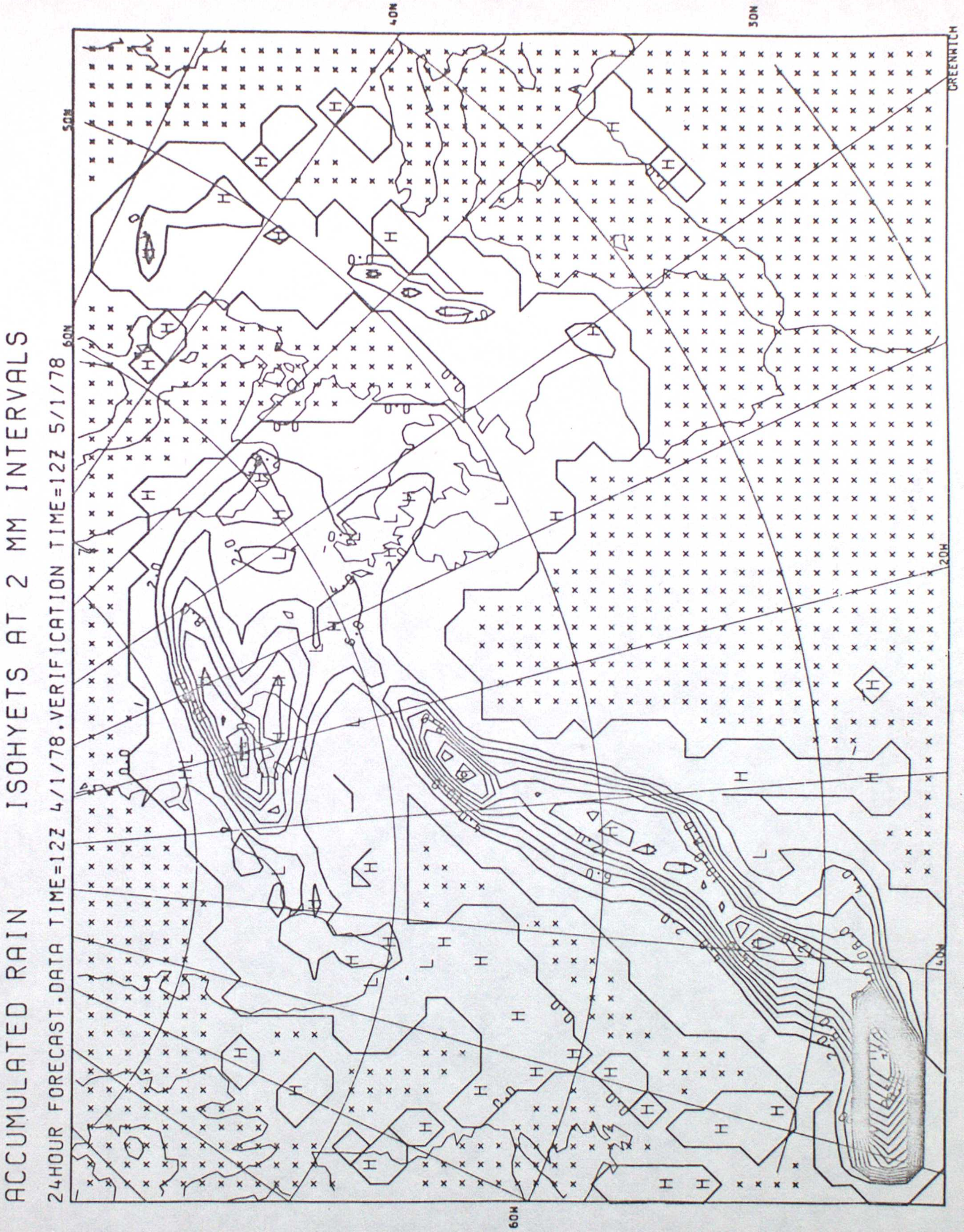
ACCUMULATED RAIN ISOHYETS AT 2 MM INTERVALS
24HOUR FORECAST.DATA TIME=12Z 4/1/78.VERIFICATION TIME=12Z 5/1/78
40N
30N
50N
60N
20N
40W
60W
GREENWICH

FIGURE 5d

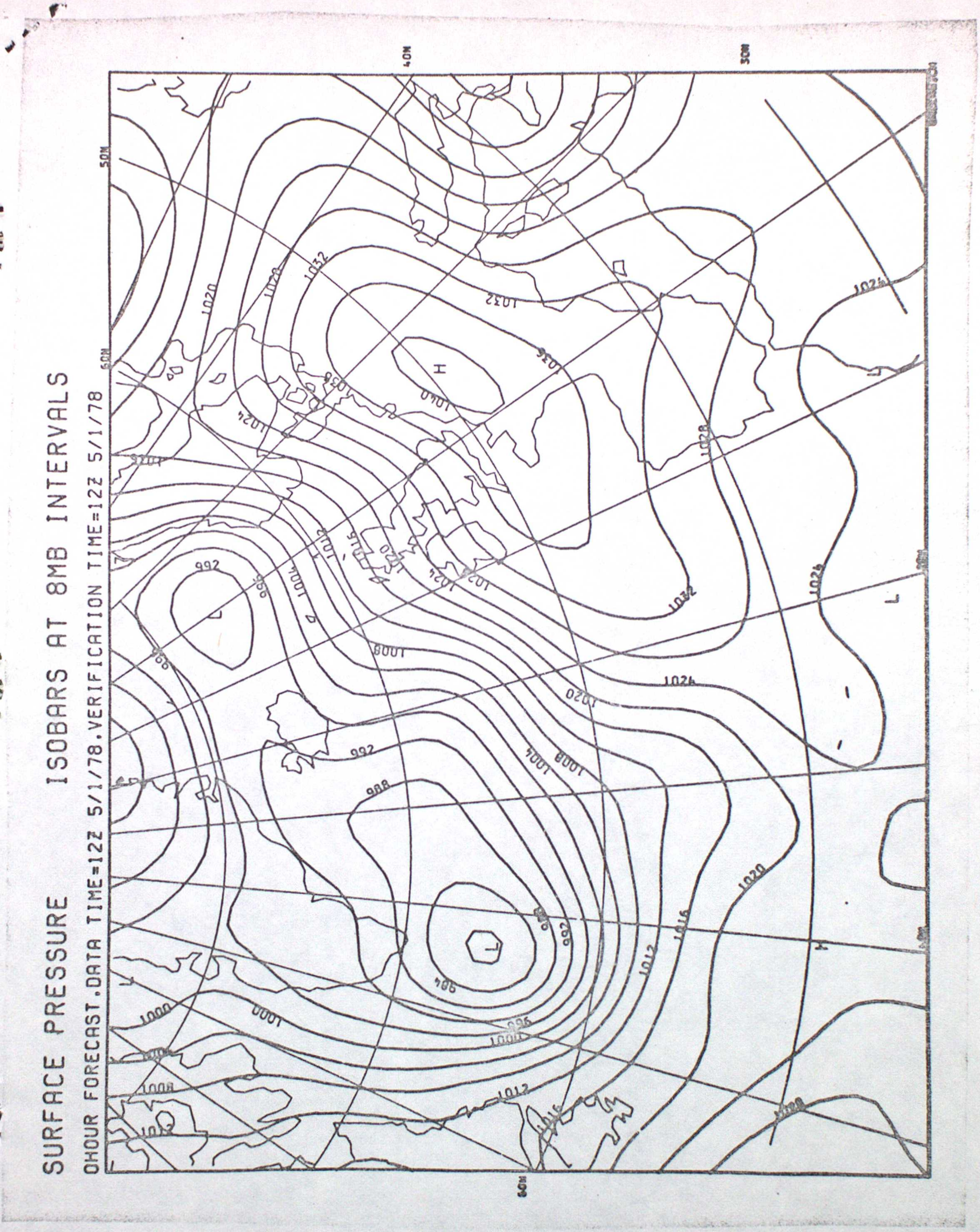
SURFACE PRESSURE ISOBARS AT 8MB INTERVALS
0HOUR FORECAST.DATA TIME=12Z 5/1/78.VERIFICATION TIME=12Z 5/1/78

FIGURE 6.